Role of implantation-induced defects on the response time of semiconductor saturable absorbers

H. H. Tan[a] and C. Jagadish
Department of Electronic Materials Engineering, Research School of Physical Sciences and Engineering, The Australian National University, Canberra, A.C.T. 0200, Australia

M. J. Lederer and B. Luther-Davies
Laser Physics Center, Research School of Physical Sciences and Engineering, The Australian National University, Canberra, A.C.T. 0200, Australia

J. Zou and D. J. H. Cockayne
Australian Key Center for Electron Microscopy and Microanalysis, University of Sydney, Sydney, N.S.W. 2002, Australia

M. Haiml, U. Siegner, and U. Keller
Institute of Quantum Electronics, Swiss Federal Institute of Technology, ETH Hönggerberg-HPT, CH-8093 Zürich, Switzerland

(Received 15 March 1999; accepted for publication 13 July 1999)

Arsenic ion implantation with thermal annealing was used to shorten the response times of GaAs-based saturable absorber structures. Ultrafast absorption bleaching measurements indicated that the recovery time was decreased with increasing the implantation dose. However, above a certain dose the recovery time increased again. This behavior was correlated with the microstructure of the residual implantation defects. © *1999 American Institute of Physics.*
[S0003-6951(99)04936-0]

Semiconductor saturable absorbers play an important role in applications such as passive mode locking[1,2] and all-optical switching.[3] In these cases, (sub)- ps response times are required whilst maintaining the highest possible modulation depth and nonlinearlity. Although GaAs and InGaAs based heterostructures grown at low temperatures (LT) by molecular-beam epitaxy can display ultrafast response times,[4,5] these materials often suffer from strongly depressed modulation, most likely due to optical transitions from the deep levels.[6] It has been shown previously that ion implantation can create fast carrier lifetimes in GaAs and InP,[7–11] and offer[5] an alternative to LT materials. However, in some of these reports, the dose dependence of the carrier lifetimes were contradictory, primarily due to the lack of effort in correlating the type of defects with the carrier lifetimes. In some cases, no saturation in the shortening of the carrier lifetimes was observed,[7,8] in another case a lower limit of 0.5 ps was reported[9] and yet in a further report, there was no clear trend.[10] To further understand the mechanism of implantation-induced shortening of the carrier lifetime, systematic structural analysis, and correlation with the optical response behavior is required. This letter reports the effect of the implantation dose and the nature of residual defects on the optical response behavior of saturable absorbers.

The structure was grown by metalorganic chemical-vapor deposition, consisting of 25 pairs of $Al_{0.15}Ga_{0.85}As$/AlAs distributed Bragg reflector (DBR) followed by 0.5 μm GaAs absorber layer. All layers were undoped and grown on semi-insulating GaAs substrates at 750 °C. The DBR had a central wavelength of 830 nm and a measured reflectivity in excess of 99%. The wafer was then implanted with 700 keV As^+ ions at room temperature to various doses. The energy of the ions was chosen so that the atomic displacement profile lay solely in the GaAs absorber layer. After implantation, the samples were annealed under an arsine ambient at 600 °C for 20 min. Finally, an antireflection (AR) coating was applied to avoid Fabry–Perot effects, since all optical measurements were done in the reflection mode.

In order to determine the temporal response of the samples we have employed a standard pump-probe technique using a 830 nm, 100 fs pulse train from a mode-locked Ti:sapphire laser. Due to the AR coating, the signals were dominated by absorption bleaching in the GaAs absorber layer. An effective recovery time, τ_A, was then defined as the delay at which the signal had fallen to $1/e$ of its peak value. Structural analysis was carried out using Rutherford backscattering-channeling (RBS–C) technique. Selected samples were then analyzed by cross-sectional transmission electron microscopy (XTEM).

Figure 1 shows τ_A as a function of implantation dose. In the unimplanted sample, the recovery time was about 17 ps (not shown). A faster recovery time was observed after implantation, indicating that additional defect states were introduced which shortened the absorber recovery times. With increasing implantation dose, more defects were expected, and hence, faster recovery time. However, with a further increase in the implantation dose ($\geqslant 1\times10^{14}$ cm^{-2}), a gradual increase in the recovery time was observed. Thus, there existed an optimum implantation dose where τ_A was minimum (τ_m). At both higher and lower doses, the recovery times began to increase from τ_m although they were still much shorter than that of the unimplanted sample. However,

[a]Electronic mail: hoe109@rsphysse.anu.edu.au

 © 1999 American Institute of Physics

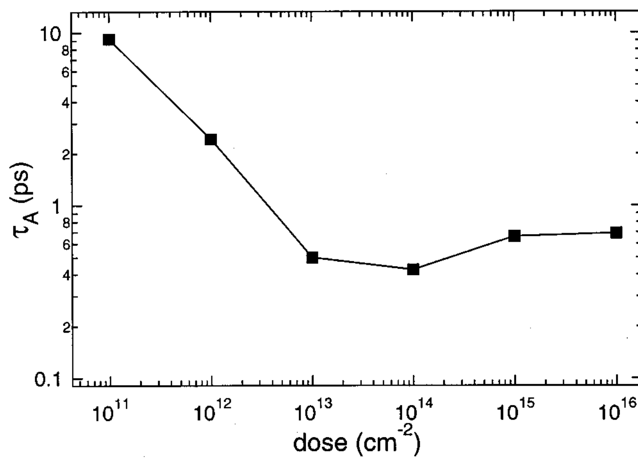

FIG. 1. Effective carrier recovery time (τ_A) plotted against the implantation dose. All samples have been annealed at 600 °C, 20 min.

the rate of increase (slope of curve) was very different between lower and higher doses. At lower doses the rate was significantly higher than that at higher doses. This difference suggests that the nature of the defects plays a significant role in the absorber recovery time.

To correlate the nature of these defects with the absorber recovery time, the results of RBS–C analysis are shown in Figs. 2(a) and 2(b) for the as-implanted (unannealed) and annealed samples, respectively. At the lowest dose (1×10^{13} cm^{-2}), a slight increase in the backscattered yield with respect to the unimplanted spectrum is noted, indicating that the implantation damage was mainly due to displaced lattice atoms and the buildup of point defects. In the case of 1×10^{14} cm^{-2}, the backscattered yield reaches that of the random level in the region of the peak of damage distribution. The damage accumulation has resulted in the agglomeration of these point defects into defect clusters which eventually overlap, resulting in the formation of a buried amorphous layer.[12–14] Indeed, the XTEM micrograph of Fig. 3(a) shows that a buried amorphous layer was formed, sandwiched between two heavily defective bands of crystalline material. As the implantation dose was increased to 1×10^{15} cm^{-2}, a continuous amorphous layer was formed, extending up to the surface, as is shown by the XTEM micrograph of Fig. 3(b). However, a narrow crystalline layer could still be observed at the bottom of the absorber layer. A further increase in the dose (1×10^{16} cm^{-2}) resulted only in an amorphous layer which extended further into the absorber layer as indicated by the RBS–C results.

Upon annealing, the sample implanted with 1×10^{13} cm^{-2} had recovered extremely well to almost the unimplanted quality (as seen in the RBS–C spectrum). In the case of 1×10^{14} cm^{-2}, fairly good damage recovery was obtained where the dechanneling level was only slightly higher than that of the unimplanted sample towards the end-of-range of the ions. An XTEM image of this sample is shown in Fig. 3(c), in which small defect clusters and dislocation loops are observed. Thus, the buried amorphous layer and the bands of the defective crystalline material had recrystallized leaving these residual defects. The recrystallization was quite efficient in this case due to the presence of two regrowth fronts (buried amorphous layer). However, for the 1×10^{15} cm^{-2}

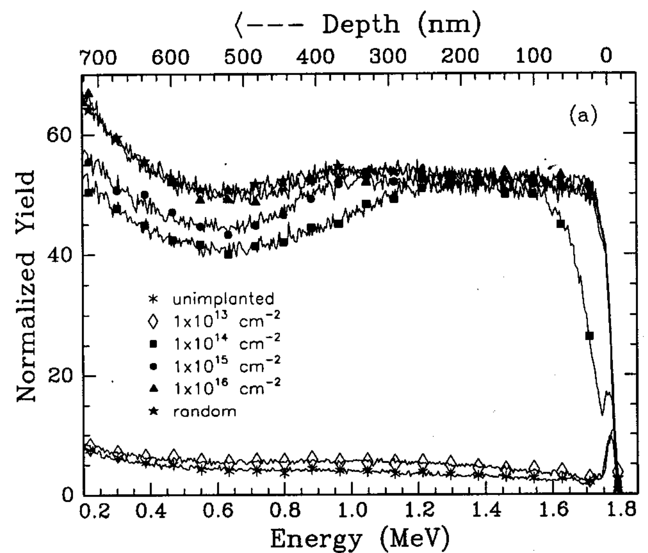

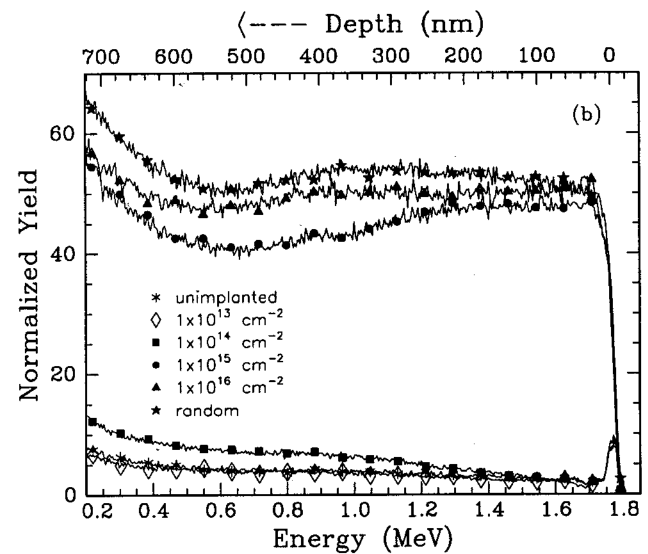

FIG. 2. (a) RBS–C spectra for samples implanted at various doses and (b) the same sample annealed at 600 °C, 20 min. the unimplanted (aligned) and random spectra are also plotted in both cases for reference.

sample, the backscattered yield had dropped to below the random level but was still quite pronounced; an indication of poor recrystallization. The XTEM image [Fig. 3(d)] shows that annealing of this sample resulted in the formation of a continuous polycrystalline layer (extending from the surface) followed by a region of dislocation loops.

The results confirmed that ion implantation is able to achieve fast recovery time (or carrier lifetimes) in GaAs as shown previously.[7–11] However, unlike some previous work,[7–10] annealing was carried out in this study. We observed a decrease in the recovery time as the implantation dose was increased. At low doses, the defect density in the absorber layer was low, mainly in the form of displaced atoms, point defects, and small clusters. Damage recovery at low doses was efficient, and hence, there were less defect states in the band gap for carrier capturing. With increasing the dose, more defects were introduced and remained after annealing, decreasing the carrier lifetime. However, if an amorphous layer was formed, the amount of residual disorder after recrystallization increases with increasing initial

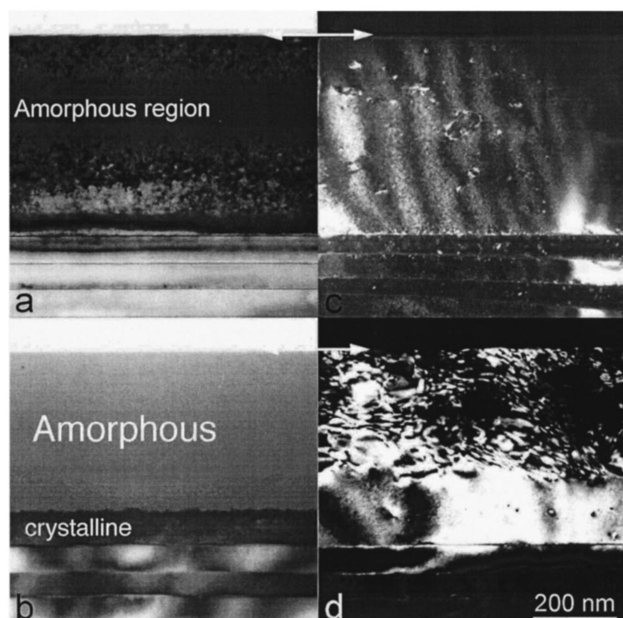

FIG. 3. XTEM images for samples implanted to doses of 1×10^{14} cm^{-2} [(a): as-implanted, (c): annealed] and 1×10^{15} cm^{-2} [(b): as-implanted, (d): annealed]. Arrowheads indicate the surface.

amorphous thickness.[13,15,16] A shortening of the recovery time of the saturable absorbers down to ~400 fs was achieved for the sample with thin amorphous layer where the residual defects were predominantly dislocation loops and clusters. Although the shortest recovery time in this study was found in the sample with dislocation loops and clusters, it is unlikely that these defects were the main cause of further reduction in the recovery times. We have previously shown that in ion implanted materials, point defects are the main cause of the shortening of carrier lifetimes.[17,18] These studies have shown that point defects were indeed present in the GaAs after implantation and annealing, although the XTEM was not able to detect them. In fact, the *rate* of reduction in recovery time (sloe of curve) from 1×10^{13} to 1×10^{14} cm^{-2} in Fig. 1 was much smaller compared to that at lower doses ($<1\times10^{13}$ cm^{-2}). This is further evidence that point defects are the main cause of shortening carrier lifetimes, since the formation of dislocation loops and defect clusters consumes point defects. It is a possibility that these point defects are As antisites although not evident in this work. Further work is underway to address this issue. XTEM results also did not reveal the presence of As precipitates, which were reported to be present after high dose implantation and annealing.[19–21] However, it should be noted that 700 keV As was used in the present work in contrast with 200 keV As used in those studies. The effect of the higher energy implant is that the As ions are spread over larger depth (volume), and hence, the local concentration of As is not high enough to form precipitates during annealing.

In contrast to previous studies where low energy As was used,[19–21] perfect recrystallization starts to break down the thicker the amorphous layer. Indeed, recrystallization of a ~373-nm-thick continuous amorphous layer [Fig. 3(b)] resulted in polycrystalline material. The polycrystals gradually increased the carrier lifetimes. It is evident from these results that what is important in shortening the recovery times is not only the concentration of defects but also the nature/type of defects in GaAs such as point defects, defect clusters, dislocation loops, and polycrystalline material, listed in the order of their effectiveness in carrier capturing.

In summary, we have demonstrated that ion implantation and annealing could shorten the response time of semiconductor saturable absorbers. We have also identified that both the concentration and type of residual defects determines the ultimate shortening of the carrier lifetime. Our results demonstrate that high implantation doses, which lead to amorphization, poor recrystallization, and polycrystalline layers after annealing, should be avoided since the response time is increased under these conditions.

H.H.T. and J.Z. would like to thank the Australian Research Council for the fellowship support. M. J. L. acknowledges the support of Electro Optic Systems Pty. Ltd. and the Australian government for the award of an APA Industry scholarship. The work (optical measurements) at ETH Zurich was supported by the Swiss National Science Foundation.

[1] U. Keller, D. A. B. Miller, G. D. Boyd, T. H. Chiu, J. F. Ferguson, and M. T. Asom, Opt. Lett. **17**, 505 (1992).
[2] U. Keller, K. Weingarten, F. Kärtner, D. Kopf, B. Braun, I. Jung, R. Fluck, C. Hönninger, N. Matuschek, and J. Aus der Au, IEEE J. Sel. Top. Quantum Electron. **2**, 435 (1996).
[3] R. Takahashi, Y. Kawamura, and H. Iwamura, Appl. Phys. Lett. **68**, 5 (1996).
[4] S. Gupta and J. F. Whitaker, IEEE J. Quantum Electron. **28**, 2464 (1992).
[5] A. C. Warren, J. M. Woodall, J. L. Freeouf, D. Grischkowsky, M. R. Melloch, and N. Otsuka, Appl. Phys. Lett. **57**, 1331 (1990).
[6] M. Haiml, U. Siegner, F. Morier-Genoud, U. Keller, M. Luysberg, P. Specht, and E. R. Weber, Appl. Phys. Lett. **74**, 1269 (1999).
[7] M. B. Johnson, T. C. McGill, and N. G. Paulter, Appl. Phys. Lett. **54**, 2424 (1989).
[8] K. F. Lamprecht, S. Juen, L. Palmtshofer, and R. A. Höpfel, Appl. Phys. Lett. **59**, 926 (1991).
[9] M. Lambsdorff, J. Kuhl, J. Rosenzweig, A. Axmann, and Jo. Schneider, Appl. Phys. Lett. **58**, 1881 (1991).
[10] F. Ganikhonov, G.-R. Lin, W.-C. Chen, C.-S. Chang, and C.-L. Pan, Appl. Phys. Lett. **67**, 3465 (1995).
[11] A. Krotkus, s. Marcinkevicius, J. Jasinski, M. Kaminska, H. H. Tan, and C. Jagadish, Appl. Phys. Lett. **66**, 3304 (1995).
[12] H. H. Tan, C. Jagadish, J. S. Williams, J. Zou, D. J. H. Cockayne, and A. Sikorski, J. Appl. Phys. **77**, 87 (1995).
[13] D. K. Sadana, Nucl. Instrum. Methods Phys. Res. B **7/8**, 375 (1985).
[14] E. Wendler, W. Wesch, and G. Götz, Nucl. Instrum. Methods Phys. Res. B **63**, 47 (1992).
[15] M. G. Grimaldi, B. M. Paine, M. A. Nicolet, and D. K. Sadana, J. Appl. Phys. **52**, 4038 (1981).
[16] C. Licoppe, Y. Nissim, C. Meriadec, and P. Krauz, J. Appl. Phys. **60**, 1352 (1986).
[17] H. H. Tan, C. Jagadish, K. P. Korona, J. Jasinski, M. Kaminska, R. Viselga, S. Marcinkevicius, and A. Krotkus, IEEE J. Sel. Top. Quantum Electron. **2**, 630 (1996).
[18] C. Jagadish, H. H. Tan, J. Jasinski, M. Kaminska, M. Palczewska, A. Krotkus, and S. Marcinkevicius, Appl. Phys. Lett. **67**, 1724 (1995).
[19] A. Claverie, F. Namavar, and Z. Lilienthal-Weber, Appl. Phys. Lett. **62**, 1271 (1993).
[20] Z. Lilienthal-Weber, F. Namavar, and A. Claverie, Ultramicroscopy **52**, 570 (1993).
[21] G.-R. Lin, W.-C. Chen, C.-S. Chang, S.-C. Chao, K.-H. Wu, T. M. Hsu, W. C. Lee, and C.-L. Pan, IEEE J. Quantum Electron. **34**, 1740 (1998).